
A Probabilistic Approach to Self-Supervised Learning using Cyclical Stochastic Gradient MCMC

Masoumeh Javanbakhat

Digital Health-Machine Learning
Hasso-Plattner-Institute, Germany
Masoumeh.Javanbakhat@hpi.de

Christoph Lippert

Digital Health-Machine Learning
Hasso-Plattner-Institute, Germany
Christoph.Lippert@hpi.de

Abstract

In this paper we present a practical Bayesian self-supervised learning method with Cyclical Stochastic Gradient Hamiltonian Monte Carlo (cSGHMC). Within this framework, we place a prior over the parameters of a self-supervised learning model and use cSGHMC to approximate the high dimensional and multimodal posterior distribution over the embeddings. By exploring an expressive posterior over the embeddings, Bayesian self-supervised learning produces interpretable and diverse representations. Marginalizing over these representations yields a significant gain in performance, calibration and out-of-distribution detection on a variety of downstream classification tasks. We provide experimental results on multiple classification tasks on four challenging datasets. Moreover, we demonstrate the effectiveness of the proposed method in out-of-distribution detection using the SVHN and CIFAR-10 datasets.

1 Introduction

Self-supervised learning is a learning strategy where the data themselves provide the labels [Jing and Tian, 2020]. The aim of self-supervised learning is to learn useful representations of the input data without relying on human annotations [Zbontar et al., 2021]. Since they do not rely on annotated data, they have been used as an essential step in many areas such as natural language processing, computer vision and biomedicine [Jospin et al., 2022], where the data annotation is time-consuming and expensive.

Despite the notable advancements made in recent years, self-supervised models are often trained using stochastic optimization methods which estimate the *distribution* over parameters as a *point mass*, ignoring the inherent uncertainty present in the parameter space. Remarkably, if the regularizer imposed on the model parameters is viewed as the log of a prior on the distribution of the parameters, optimizing the cost function may be viewed as a *maximum a-posteriori* (MAP) estimate of model parameters [Li et al., 2016b]. Bayesian methods provide principled alternatives that model the whole posterior over the parameters and effectively account for the inherent uncertainty in the parameter space [Zhang et al., 2020]. While the benefits of Bayesian methods and modeling uncertainty have been extensively explored in supervised learning [Li et al., 2016a, Maddox et al., 2019, Wilson and Izmailov, 2020], their potential advantages in self-supervised learning remain largely unexplored.

Indeed the posterior distribution over the parameters of a self-supervised learning model may be multimodal and thus insufficiently represented by a single point estimate. Each mode in the posterior can provide a meaningful different representation of data. By exploring the posterior distribution over the parameters instead of relying on point mass, our aim is to enhance performance and generalizability in downstream tasks. Additionally, it enables the estimation of uncertainties associated with

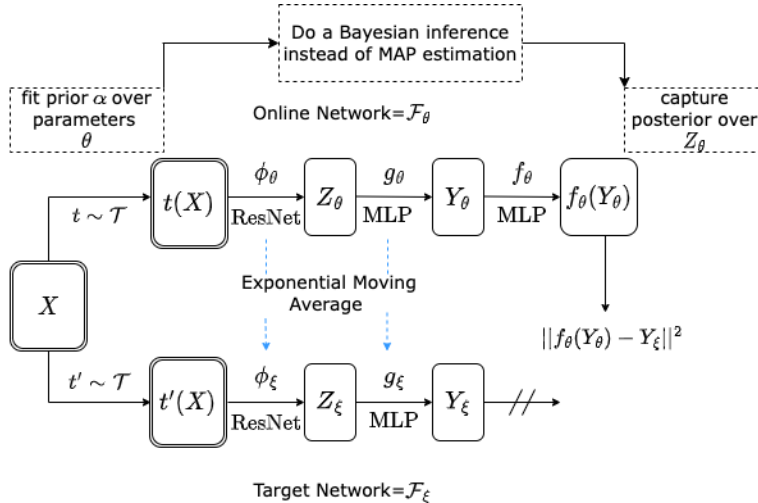


Figure 1: An illustration of Bayesian BYOL. We fit a prior over parameters of encoder. Perform Bayesian optimization instead of MAP estimation, to capture posterior over embeddings. Marginalize over embeddings in downstream task.

predictions in downstream task, which holds significant value in numerous critical decision-making systems.

Our contributions. In this paper, we propose a novel Bayesian formulation for self-supervised learning that surpasses the limitations of MAP estimation by approximating the full posterior distribution over representations. To achieve this, we leverage the power of a family of Markov Chain Monte Carlo (MCMC) [Neal, 1996] methods known as Cyclical Stochastic Gradient Hamiltonian Monte Carlo (cSGHMC) [Zhang et al., 2020], enabling us to effectively capture the multimodality inherent in the posterior distribution. Within this framework, we utilize BYOL [Grill et al., 2020], a state-of-the-art model in contrastive learning, to learn representations. Our experimental results demonstrate the remarkable potential of Bayesian learning, which unlocks enhanced performance, superior generalizability, and improved calibration in various downstream tasks, including classification and out-of-distribution detection. Importantly, our approach also enables the estimation of uncertainty in the predictive space in downstream task, a crucial aspect that has been disregarded by deterministic nature of conventional self-supervised learning methods.

2 Related Works

This work closely aligns with two lines of research: Bayesian inference and self-supervised learning.

Bayesian inference Bayesian Deep Learning evolving from Bayesian Neural Networks [Denker and LeCun, 1990, Neal, 1996] provides a compelling alternative to point estimation by capturing model uncertainty or epistemic uncertainty. Sampling the posterior distribution poses challenges in general cases, leading to the adoption of approximation methods. Among these methods, MCMC algorithms stand out as a popular choice for accurately sampling the posterior distribution, while variational inference VI [Blundell et al., 2015] offers a technique for learning an approximate posterior distribution. In recent research, Stochastic Gradient Markov Chain Monte Carlo (SG-MCMC) methods [Welling and Teh, 2011, Chen et al., 2014, Ma et al., 2015] have gained prominence for combining MCMC methods with minibatching, enabling scalable inference on large datasets. Additionally, a notable advancement in this domain is the introduction of Cyclical Stochastic Gradient MCMC (cSG-MCMC) [Zhang et al., 2020]. This method specifically addresses the exploration of highly multimodal parameter spaces within realistic computational budgets [Zhang et al., 2020].

Self Supervised Learning Self-supervised learning plays a crucial role in acquiring valuable representations from a vast amount of unlabeled data, leading to improved performance in downstream

tasks. It is widely recognised as a pivotal step toward developing more capable and data-efficient learning systems [Von Kügelgen et al., 2021]. Among the promising approaches in self-supervised learning, contrastive methods [Chen et al., 2020] stand out. These methods learn representations by maximizing the similarity between embeddings derived from different distorted versions of an image [Zbontar et al., 2021]. However, one major problem with similarity learning is feature collapse, where the learned features of the model converge to a single point in the feature space, resulting in a loss of discriminative power. To address this issue, several techniques have been proposed. For instance, in simCLR [Chen et al., 2020], the use of negative samples is introduced. Another approach, employed in BYOL [Grill et al., 2020], involves leveraging stop gradients to prevent feature collapse.

Pre-trained models as Bayesian priors There have been previous works that formulate a pretrained representation as a Bayesian prior that is optimal for data from the second task. Notably Gao et al. [2022] extend the theory of reference priors to compute an uninformative Bayesian priors by maximizing the mutual information between the task and the weights. They apply reference priors in two problems: Bayesian semi-supervised learning using unlabeled data and transfer learning, where the labeled data from the source task are utilized. In another study, Shwartz-Ziv et al. [2022] adopt a variational approach to construct an informative prior from pre-training data, aiming to maximize the performance in a single downstream task. While these approaches show promise, our method differs in several key aspects: (1) We use sampling to explore a full posterior over the representations, whereas Shwartz-Ziv et al. [2022] rely on a variational approximation centered on one of the modes of the posterior. VI is prone to overlay representation even within the mode, potentially limiting its ability to capture uncertainty accurately. (2) our approach utilizes a simple yet effective representation for the posterior distribution, requiring minimal intervention while yielding promising results across various downstream tasks. It enables accurate and reliable uncertainty quantification which is crucial in many practical applications. In [Zhang et al., 2020] authors indicate the importance of capturing different modes in the posterior in order to accurately estimate uncertainties. By addressing these differences, our proposed approach offers a novel perspective on leveraging pretrained representations in a Bayesian framework, paving the way for improved performance and reliable uncertainty estimation in diverse downstream tasks.

3 Problem Statement

Given a dataset \mathcal{D} , a self-supervised learning model \mathcal{F}_θ parameterized by θ , aims to produce a representation Z_θ by solving a predefined proxy task. In this paper we wish to learn a distribution over the embeddings Z_θ by placing a prior over the parameters θ and adopting Bayesian learning instead of relying on MAP estimation. Our method is illustrated in Fig. 1. To learn the representations, we use BYOL. In order to capture the distribution over the embeddings, we utilize cSGHMC. In the following sections, we first provide a description of the self-supervised learning model employed for representation learning. Then, we describe cSGHMC and highlight how it allows to obtain a distribution over the embeddings.

3.1 Self supervised learning

The aim of contrastive learning is to learn representations by contrasting two augmented views of an image. Particularly BYOL learns representations by reducing a contrastive loss between two neural networks referred to as online network \mathcal{F}_θ (parameterized by θ) and target network \mathcal{F}_ξ (parameterized by ξ). Each network consists of three components, an encoder $\phi(\cdot)$ (e.g., Resnet-18), a projection head $g(\cdot)$ (e.g., an MLP) and a prediction head $f(\cdot)$ (e.g., an MLP). For a given mini-batch $X = \{x_i\}_{i=1}^N$ sampled from a dataset \mathcal{D} it produces two distorted views, $t(X)$ and $t'(X)$, via a distribution of data augmentations \mathcal{T} . The two batches of distorted views then are fed to the online network and the target network respectively, producing batches of embeddings, Z_θ and Z_ξ , respectively. These features are then transformed with the projection heads into Y_θ and Y_ξ . The online network then outputs a prediction $f_\theta(Y_\theta)$ of Y_ξ using prediction head f_θ . Finally the following mean squared error between the normalized predictions $\bar{f}_\theta(Y_\theta)$ and target projections \bar{Y}_ξ is defined:

$$\mathcal{L}_{\theta,\xi} = \|\bar{f}_\theta(Y_\theta) - \bar{Y}_\xi\|^2 = 2 - 2 \cdot \frac{\langle \bar{f}_\theta(Y_\theta), \bar{Y}_\xi \rangle}{\|\bar{f}_\theta(Y_\theta)\| \cdot \|\bar{Y}_\xi\|}. \quad (1)$$

$\tilde{\mathcal{L}}_{\theta,\xi}$ is computed by separately feeding $t'(X)$ to the online network \mathcal{F}_θ and $t(X)$ to the target network \mathcal{F}_ξ . Indeed $\mathcal{L}_{\theta,\xi}$ and $\tilde{\mathcal{L}}_{\theta,\xi}$ are the same, only the views input to the target and online networks are swapped over. Then, at each training step, a stochastic optimization step is performed to minimize

$$\mathcal{L}_{\theta,\xi}^{\text{BYOL}} = \mathcal{L}_{\theta,\xi} + \tilde{\mathcal{L}}_{\theta,\xi} \quad (2)$$

The gradient is taken only with respect to θ . So, during training only the parameters θ are updated as follows:

$$\theta \leftarrow \text{optimizer}(\theta, \nabla_\theta \mathcal{L}_{\theta,\xi}^{\text{BYOL}}) \quad (3)$$

The weights ξ are an exponential moving average of the online network’s parameters θ with a target decay rate $\tau \in [0, 1]$,

$$\xi \leftarrow \tau\xi + (1 - \tau)\theta. \quad (4)$$

At the end of training, the encoder $\phi_\theta(\cdot)$ is used for the downstream task. During training only the parameters θ of the online network \mathcal{F}_θ are updated.

3.2 Posterior Sampling using cSGHMC

In the Bayesian paradigm, for a given dataset $\mathcal{D} = \{x_i\}_{i=1}^n$ and a θ -parameterized model, the following *a-posterior distribution* over θ is computed using Bayes’ rule as: $p(\theta|\mathcal{D}) \propto p(\mathcal{D}|\theta)p(\theta)$, where $p(\theta)$ is a *prior* assigned to the parameters θ and $p(\mathcal{D}|\theta)$ is the likelihood.

In MAP optimization, the prior has the role of a regularizer and the likelihood has the role of a cost function. An optimizer is optimized to find the MAP solution which is amenable to the parameter update:

$$\Delta\theta = -\frac{\ell}{2} \left(\frac{n}{N} \sum_{i=1}^N \nabla_\theta \log p(x_i|\theta) + \nabla_\theta \log p(\theta) \right) \quad (5)$$

for a given randomly sampled mini-batch $X = \{x_i\}_{i=1}^n \subset \mathcal{D}$ and learning rate ℓ .

In contrast to MAP optimization, in the Bayesian paradigm the model explores the distribution over the model parameters. Welling and Teh [2011] showed that this distribution can be approximated using Stochastic Gradient Langevin Dynamics (SGLD) by injecting Gaussian noise to the parameter updates of SGD so that they do not collapse to just the MAP solution. This leads to the following parameter update:

$$\Delta\theta = -\frac{\ell}{2} \left(\frac{n}{N} \sum_{i=1}^N \nabla_\theta \log p(x_i|\theta) + \nabla_\theta \log p(\theta) \right) + \sqrt{\ell}\epsilon, \quad \epsilon \sim \mathcal{N}(0, I) \quad (6)$$

Note that when \mathcal{D} is too large, it is too expensive to evaluate the log posterior $U(\theta) := \log p(\mathcal{D}|\theta) + \log p(\theta)$, for all the data points at each iteration. Hence, SG-MCMC methods use a mini-batch gradient to approximate $\nabla_\theta U(\theta)$ with an unbiased estimate $\nabla_\theta U(\theta) \approx n\nabla_\theta \tilde{U}(\theta)$, where $\nabla_\theta \tilde{U}(\theta) := \frac{1}{N} \sum_{i=1}^N \nabla_\theta \log p(x_i|\theta) + \frac{1}{n} \nabla_\theta \log p(\theta)$. In particular, note that the log prior *scales* with the *dataset size* at each iteration.

SGHMC [Chen et al., 2014] is an improved counterpart of SGLD which introduces a momentum variable \mathbf{m} . The posterior sampling is done using the following update rule:

$$\begin{aligned} \mathbf{m} &= \beta\mathbf{m} - \frac{\ell}{2} n \nabla_\theta \tilde{U}(\theta) + \sqrt{(1-\beta)\ell}\epsilon; \quad \epsilon \sim \mathcal{N}(0, I) \\ \theta &= \theta + \mathbf{m} \end{aligned} \quad (7)$$

where β is the momentum term. The convergence to the true posterior is ensured by Equations (6) and (7), given that learning rate ℓ follows the Robbins-Munro conditions and decays towards zero [Welling and Teh, 2011]. Zhang et al. [2020] showed that replacing the traditional decreasing learning rate schedule in SGHMC with a cyclical variant allows to explore multimodal posterior distributions and developed cSGHMC. In this paper we apply cSGHMC to take samples from the posterior distribution.

4 Posterior over Representations

To infer a posterior over the embeddings, we place a *prior* α over the parameters θ of the online network \mathcal{F}_θ . By placing a distribution over θ , we induce a distribution over an infinite space of online networks \mathcal{F}_θ . This results in a distribution over embeddings Z_θ . Sampling from this distribution corresponds to sampling from the following conditional posterior:

$$p(\theta|X) \propto p(X|\theta)p(\theta|\alpha), \quad (8)$$

where X is a mini-batch. Equation (8) can be interpreted intuitively as follows. We sample weights θ from the prior $p(\theta|\alpha)$. By conditioning on this sample of weights, we construct a specific online network \mathcal{F}_θ . This network is then utilized to generate an embedding Z_θ by minimizing the loss function $\mathcal{L}_{\theta,\xi}^{\text{BYOL}}$.

Implementation Details. In practice, when considering the online network $\mathcal{F}_\theta(X) = f_\theta \circ g_\theta(\phi_\theta(t(X)))$, applied on a mini-batch X transformed using data augmentation $t \sim \mathcal{T}$, we place a prior α on the parameters θ of the encoder ϕ_θ . As a prior α , we assume isotropic Gaussian distribution $\mathcal{N}(0, I)$. Subsequently, we compute $p(X|\theta) = \|f_\theta(Y_\theta) - Y_\xi\|^2$ and $\tilde{U}(\theta) = \log p(X|\theta) + \frac{1}{n} \log p(\theta|\alpha)$.¹ Note that Zimmermann et al. [2021] indicated that contrastive learning inverts the data generating process and investigated the connection between contrastive learning and identifiability in the form of nonlinear Independent Components Analysis (ICA). Specifically, they showed that contrastive loss can be interpreted as the cross entropy between the (conditional) ground-truth and inferred latent distribution [Zimmermann et al., 2021]². This implies that considered loss can be interpreted as a negative log-likelihood, and by utilizing cSGHMC, we can efficiently obtain samples from the posterior using the update rule described in Equation (7). Our proposed method for sampling from the posterior distribution over embeddings Z_θ is outlined in Algorithm 1. The algorithm generates samples from the posterior over the parameters θ of the online network \mathcal{F}_θ . This yields a distribution over embeddings Z_θ , as we compute the gradients of the loss with respect to the sampled parameters θ .

Wenzel et al. [2020] indicated that tempering helps improve performance for Bayesian inference where $p(\theta|\mathcal{D}) \propto \exp(-U(\theta)/T)$, and $T < 1$ is a temperature. Here we also use cold posterior and choose T by tuning on validation set. More details can be found in Appendix A.

Our proposed probabilistic approach represents a natural Bayesian extension of MAP optimization, encompassing the advantages of uncertainty estimation. In fact, by performing MAP optimization using SGD in Algorithm 1 instead of posterior sampling, one approximates the entire *posterior* distribution over θ with a single *point estimate*, thus disregarding the richness of the full posterior.

Algorithm 1 Probabilistic Self-Supervised Learning

Require: ℓ initial learning rate, β momentum term, K number of training iterations

Ensure: sequence $\theta^1, \theta^2, \dots$

for $k = 1 : K$ **do**

 sample mini-batch $X = \{x_i\}_{i=1}^N$ and augmentations $t \sim \mathcal{T}, t' \sim \mathcal{T}$

 compute $\tilde{U}(\theta)$ for mini-batch X

$\ell \leftarrow C(k)\ell$

\triangleright update learning rate using cyclic modulation

$\mathbf{m} \leftarrow \beta\mathbf{m} - \frac{\ell}{2}n\nabla_\theta\tilde{U}(\theta) + \sqrt{T(1-\beta)}\ell\epsilon$

$\epsilon \sim \mathcal{N}(0, I)$

$\theta \leftarrow \theta + \mathbf{m}$

\triangleright update parameters θ using Equation (7)

$\xi \leftarrow \tau\xi + (1-\tau)\xi$

if end of cycle **then**

 yield θ

end if

end for

Marginalizing over representations: After completing the pre-training phase, we can proceed to marginalize the posterior distribution over θ for downstream tasks. To compute the predictive

¹For simplicity of notations we ignore normalization and symmetrization

²For a more detailed and precise discussion on this matter, we refer to Zimmermann et al. [2021]

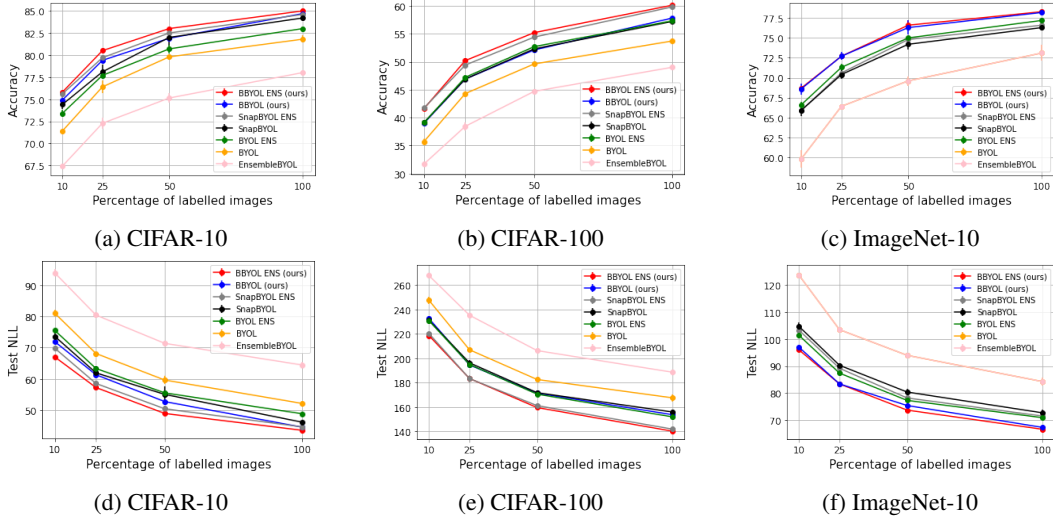


Figure 2: Performance comparison. First row indicates improvement in accuracy. The second row indicates improvement in calibration. Bayesian approaches outperform MAP estimation in terms of both accuracy and calibration. We use pre-trained model on STL-10 for CIFAR-10 and CIFAR-100. For ImageNet-10, a pre-trained model on Tiny-ImageNet is used.

distribution for a new instance x^* we use a model average over all collected samples with respect to the posterior over θ .

$$p(y^*|x^*, \mathcal{D}) = \int p(y^*|x^*, \theta)p(\theta|\mathcal{D})d\theta \approx \frac{1}{S} \sum_{s=1}^S p(y^*|x^*, \theta^{(s)}), \theta^{(s)} \sim p(\theta|\mathcal{D}) \quad (9)$$

We will observe that this model average significantly enhances performance, calibration, and out-of-distribution detection in downstream tasks. Additionally, by possessing samples from the posterior, we can compute the entropy for a given instance x^* , thereby providing an estimation of uncertainty in the predictive space:

$$\mathcal{H}(y^*|x^*, \mathcal{D}) = - \sum_{c \in \mathcal{C}} p(y^*|x^*, \mathcal{D}) \log p(y^*|x^*, \mathcal{D})$$

5 Experiments

In this section, we present our experimental results. We evaluate the performance and efficiency of the proposed method on several tasks including semi-supervised learning and out-of-distribution detection. First, we describe our experimental setup. Then, we evaluate our model using semi-supervised setting, and lastly, we evaluate our model using out-of-distribution examples. We implemented the code in PyTorch [Paszke et al., 2017] and the link to our code is available in the supplementary material.

5.1 Experimental Setup

Datasets For pre-training phase, we pre-train all models on two image datasets STL-10 [Coates et al., 2011] and Tiny-ImageNet [Le and Yang, 2015]. For STL-10, its 100,000 unlabeled samples are used for pre-training. For downstream task we conduct our experiments on four image classification datasets: CIFAR-10, CIFAR-100 [Krizhevsky and Hinton, 2009], STL-10 and ImageNet-10 [Chang et al., 2017]. A brief description of these datasets is summarized in Table 1. For all datasets pre-trained models are fine-tuned on Train set and evaluated on Test set, except for ImageNet-10 that the Validation set is used for evaluation, since the Test set of this dataset dose not have ground-truth labels.

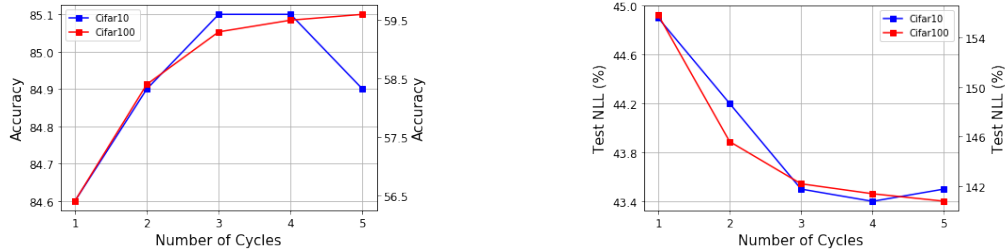


Figure 3: The effect of ensemble size on CIFAR-10 and CIFAR-100 in BBYOL ENS: (a) Testing accuracy (%) (b) Testing NLL (%) as a function of the number of cycles. Adding more embeddings improves accuracy and calibration.

Implementation Details We adopt ResNet-18 [He et al., 2016] as an encoder for the self-supervised learning model. Following the original setting of BYOL, we use 2-layer MLPs as the projection and prediction heads. We apply the standard ResNet without modification on the input images of original sizes for all datasets given in Table 1 which produces a feature vector of size 512 for each sample. We refer this feature vector as *representation* or *embedding*. We use the same set of data augmentations in Grill et al. [2020] on both datasets for pre-training, consists of random cropping and resizing with a random horizontal flip, followed by a color distortion and a grayscale conversion.

Evaluation Metrics Two widely-used metrics including Accuracy (ACC), and Negative Log Likelihood (NLL) are utilized to evaluate our method. Higher value of ACC indicates better performance of the model and lower value of NLL indicates better calibration.

Baselines In order to demonstrate the effectiveness of our proposed probabilistic approach we conduct a comparative analysis with several methods including: (i) BYOL: MAP estimation trained with SGD; (ii) BYOL ENS: stochastic optimization ensemble method; (iii) SnapBYOL: MAP estimation trained with SGD and cyclical stepsize schedule; (iv) SnapBYOL ENS: a stochastic optimization ensemble method with a cyclical stepsize schedule and (v) EnsembleBYOL: an ensemble of BYOL trained with SGD from scratch for different random initialization. In the aforementioned methods, when we utilize only the last embedding in downstream task we refer to the model as BYOL, SnapBYOL and BBYOL. However, when we perform marginalization over embeddings, we adopt BYOL ENS, SnapBYOL ENS and BBYOL ENS. It is worth nothing that EnsembleBYOL also signifies marginalizing over embeddings.

For training BYOL we employed SGD optimizer with a fixed learning rate schedule. For SnapBYOL we utilized SGD optimizer with a cyclic stepsize schedule. In training BBYOL, we followed the training procedure outlined in Algorithm 1, where we use a cyclic stepsize schedule [Zhang et al., 2020] with cycle length of 50. All models are trained from scratch for 1000 epochs. In BBYOL and SnapBYOL, we collect 1 sample at the end of each cycle for the last 4 cycles resulting in a total of 4 samples. In BYOL, we take 4 samples on last 200 epochs, maintaining a regular interval of 50 epochs between each sample. To ensure consistency in the training budget across all methods, we trained EnsembleBYOL by employing the SGD optimizer with a fixed learning rate for 250 epochs, using four different random seeds. The curve in the plot indicates marginalizing over 4 embeddings. Other training and baseline hyperparameters are provided in Appendix A.

Table 1: A summary of datasets used for evaluations.

Dataset	Split	Samples	Classes
CIFAR-10	Train+Test	60000	10
CIFAR-100	Train+Test	60000	100
STL-10	Train+Test	13000	10
ImageNet-10	Train+Validation	13000	10

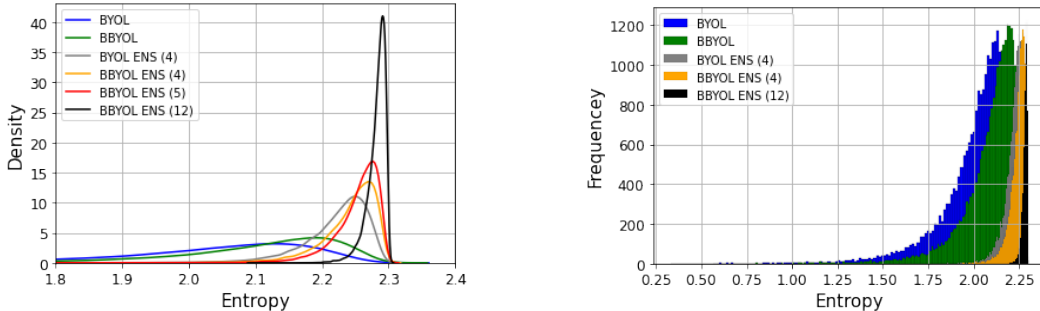


Figure 4: Histogram of the predictive entropy on test examples from unknown data (SVHN), as we vary the ensemble size.

The experiments are carried out on Nvidia A40 48 GB and it takes about 21 gpu-hours on STL-10, and 24 gpu-hours on Tiny-ImageNet. We repeat experiments for 3 random seeds and report average NLL and ACC over 3 runs with the standard error from the mean predictor.

5.2 Image Classification

In this section we present the evaluation results of proposed method on a semi-supervised image classification task. In this task, the quality of learned representations are assessed by fine-tuning a pre-trained model on subsets of original training datasets with labels. We evaluate over a variety of downstream training set sizes and analyze the obtained gains in performance and calibration. We follow the semi-supervised protocol in [Grill et al., 2020] and provide a detailed description of hyperparameters in Appendix A.

In Figure 2, we compare the above described methods across various dataset sizes in terms of accuracy and calibration. We observe the followings: (i) BBYOL consistently outperforms BYOL and SnapBYOL in all datasets in both metrics (the improvement of BBYOL over SnapBYOL in CIFAR-100 is relatively modest). (ii) Marginalizing over representations in BBYOL ENS improves performance and calibration compared to BBYOL. Marginalizing is more effective when the downstream task is more difficult for example in CIFAR-100. (iii) Marginalizing over representations in BYOL ENS and SnapBYOL ENS also improves performance. It is due to the nature of contrastive loss which induces diversity in the parameter space. Whenever the loss is not too high, marginalizing over these representations contributes to enhanced performance. However, even with this improvement, BBYOL ENS still achieves sizable gains in both performance and calibration over the baselines. (iv) Marginalizing is relatively more valuable on intermediate dataset sizes.

Among above observations, Point (i) is particularly interesting, even if we do not want to use model averaging over representations due to a higher test-time cost, the last representation in a BBYOL trained using a Bayesian approach has significant better performance in accuracy and calibration compared to a MAP estimation. In Appendix B we provide additional evaluations with models pre-trained on Tiny-ImageNet.

Ensemble Size In some applications, it may be beneficial to vary the size of the ensemble dynamically at test time depending on available resources. Figure 3 displays the performance of BBYOL ENS on CIFAR-10 and CIFAR-100 datasets as the effective ensemble size, is varied. Although ensembling more models generally gives better performance, we observe significant gains in accuracy and drops in NLL when the second and third models are added to the ensemble. In most cases, an ensemble of two models outperforms the baseline model. In CIFAR-10, we have noticed a decline in performance upon introducing the fifth representation. This decrease can be attributed to the relatively high loss of this particular model, indicating that it may not be suitable for ensembling. Therefore, we utilize the representations from the last four cycles in CIFAR-10 and CIFAR-100 for ensembling.

Table 2: Results for OOD detection for various settings. Numbers in parentheses indicate number of embeddings. BBYOL ENS constantly outperforms all other methods for various number of ensembles. Underlined results indicate the results of our method and best results are in **bold face**.

In-Distribution	Out-of-Distribution	Method	NLL ↓	AUROC (%) ↑
CIFAR-100	SVHN	BYOL	2.61 ± 0.0	84.1 ± 1.7
		BBYOL	<u>2.53</u> ± 0.0	<u>89.6</u> ± 0.7
		BYOL ENS (4)	2.38 ± 0.0	93.6 ± 0.4
		BBYOL ENS (4)	<u>2.36</u> ± 0.0	<u>95.7</u> ± 0.1
		BYOL ENS (5)	2.37 ± 0.0	94.8 ± 0.3
		BBYOL ENS (5)	<u>2.35</u> ± 0.0	<u>96.4</u> ± 0.1
		BBYOL ENS (12)	2.32	98.3
CIFAR-100	CIFAR-10	BYOL	2.62 ± 0.02	84.3 ± 1.4
		BBYOL	<u>2.53</u> ± 0.0	<u>89.4</u> ± 0.5
		BYOL ENS (4)	2.38 ± 0.0	93.6 ± 0.3
		BBYOL ENS (4)	<u>2.37</u> ± 0.0	<u>95.8</u> ± 0.2
		BYOL ENS (5)	2.37 ± 0.01	94.8 ± 0.3
		BBYOL ENS (5)	<u>2.35</u> ± 0.0	<u>96.4</u> ± 0.1
		BBYOL ENS (12)	2.31	98.2

5.3 Out-of-Distribution Detection

To further analyze the effectiveness of the proposed probabilistic approach compared to the MAP estimation, we consider the out-of-distribution (OOD) detection task [Zhang et al., 2020]. In this task, a model trained on known data is evaluated on unseen data. For the unseen data, we expect the model indicates low probability and max entropy [Zhang et al., 2020]. It implies that the mode of the predictive entropy’s histogram focuses at higher value. Moreover, we assess the quality of the predictive uncertainty using two quantitative metrics, NLL and the area under the receiver operating characteristic curve (AUROC) [Deng et al., 2009], a higher value of AUROC indicates a better detector.

We consider two datasets CIFAR-10 and SVHN [Netzer et al., 2011] as OOD datasets. A pre-trained model on STL-10, is fine-tuned on CIFAR-100 and evaluated on SVHN and CIFAR-10. Figure 4 presents the histogram of the predictive entropy for SVHN (out-of-distribution). The histogram of the predictive entropy for CIFAR-10 had the same distribution, so we just included SVHN.

We see that the uncertainty estimates from BBYOL and BBYOL ENS are better than the other methods, as the mode of histogram focuses at higher values. BYOL ENS also improves uncertainty estimate on unseen data compared to BYOL but still achieves less entropy than BBYOL ENS. Moreover the predictive uncertainty improves on unseen data, as the ensemble size increases reaching to the highest value in BBYOL ENS (12), where we take 12 samples from last 4 cycles (3 samples per cycle). It indicates that embeddings produced by sampling from the posterior in BBYOL come from different modes and provide different characterization of training data. When testing on unseen data, each mode provides different predictions on unseen data leading to max disagreement and higher entropy.

We also report the quantitative results for NLL and AUROC in Table 2 as the ensemble size is varied. BBYOL ENS (5) indicates marginalizing over 5 embeddings collected from last 5 cycles. Consistent with our previous results BBYOL improves BYOL in terms of both calibration (lower NLL) and AUROC (higher) by large margin (5.5% in AUROC only for last embedding and 14.2% when we marginalize over 12 embeddings). The improvement in calibration and AUROC consistently increases by increasing the number of ensemble size.

6 Conclusion

In this paper, we propose a novel approach that challenges the traditional Maximum A Posteriori (MAP) solution for learning representations, advocating instead for the utilization of Bayesian methods. Our primary objective is to thoroughly explore the posterior distribution over the representations and investigate the potential advantages offered by incorporating probabilistic sampling techniques

into representation learning. By deviating from the traditional MAP approach, we aim to shed light on the extensive benefits and valuable insights that can be gained from embracing Bayesian approaches in representation learning. To achieve this, we employ a powerful SG-MCMC method designed to capture the multi-modal posterior distribution. Through extensive experiments, we have obtained compelling findings that underscore the distinctiveness of samples derived from the posterior distribution. This distinctiveness translates into remarkable improvements across multiple metrics, including accuracy, calibration, and uncertainty estimation, in downstream tasks. By embracing the richness of the posterior, we empower models to better capture the inherent complexity and nuances of the underlying data.

7 Broader Impact

Incorporating Bayesian approaches into self-supervised learning has the potential to significantly impact the field across multiple dimensions. One prominent advantage is the ability to introduce the concept of uncertainty, not only in the predictive space but also in the embedding space. Exploring the relationship between these two forms of uncertainty presents an intriguing avenue for analysis, offering valuable insights into their interplay and potential implications. Understanding how uncertainty manifests in both prediction and embedding spaces can contribute to a more comprehensive understanding of the underlying data and enhance the robustness and reliability of self-supervised learning algorithms.

References

- C. Blundell, J. Cornebise, K. Kavukcuoglu, and D. Wierstra. Weight uncertainty in neural network. In *International conference on machine learning*, pages 1613–1622. PMLR, 2015.
- J. Chang, L. Wang, G. Meng, S. Xiang, and C. Pan. Deep adaptive image clustering. In *Proceedings of the IEEE international conference on computer vision*, pages 5879–5887, 2017.
- T. Chen, E. Fox, and C. Guestrin. Stochastic gradient hamiltonian monte carlo. In *Proceedings of the 31st International Conference on Machine Learning*, volume 32, pages 1683–1691. PMLR, 2014.
- T. Chen, S. Kornblith, M. Norouzi, and G. Hinton. A simple framework for contrastive learning of visual representations. In *International conference on machine learning*, pages 1597–1607. PMLR, 2020.
- A. Coates, A. Ng, and H. Lee. An analysis of single-layer networks in unsupervised feature learning. In *Proceedings of the fourteenth international conference on artificial intelligence and statistics*, pages 215–223. JMLR Workshop and Conference Proceedings, 2011.
- J. Deng, W. Dong, R. Socher, L.-J. Li, K. Li, and L. Fei-Fei. Imagenet: A large-scale hierarchical image database. In *2009 IEEE Conference on Computer Vision and Pattern Recognition*, pages 248–255, 2009.
- J. S. Denker and Y. LeCun. Transforming neural-net output levels to probability distributions. In *Proceedings of the 3rd International Conference on Neural Information Processing Systems*, page 853–859, 1990.
- Y. Gao, R. Ramesh, and P. Chaudhari. Deep reference priors: What is the best way to pretrain a model? In *Proceedings of the 39th International Conference on Machine Learning*, volume 162, pages 7036–7051. PMLR, 2022.
- J.-B. Grill, F. Strub, F. Altché, C. Tallec, P. Richemond, E. Buchatskaya, C. Doersch, B. Avila Pires, Z. Guo, M. Gheshlaghi Azar, et al. Bootstrap your own latent—a new approach to self-supervised learning. In *Advances in neural information processing systems*, volume 33, pages 21271–21284, 2020.
- K. He, X. Zhang, S. Ren, and J. Sun. Deep residual learning for image recognition. In *2016 IEEE Conference on Computer Vision and Pattern Recognition (CVPR)*, pages 770–778, 2016.

- L. Jing and Y. Tian. Self-supervised visual feature learning with deep neural networks: A survey. In *IEEE transactions on pattern analysis and machine intelligence*, volume 43, pages 4037–4058, 2020.
- L. V. Jospin, H. Laga, F. Boussaid, W. Buntine, and M. Bennamoun. Hands-on bayesian neural networks—a tutorial for deep learning users. In *IEEE Computational Intelligence Magazine*, volume 17, pages 29–48, 2022.
- A. Krizhevsky and G. Hinton. Learning multiple layers of features from tiny images. Technical Report 0, University of Toronto, 2009.
- Y. Le and X. Yang. Tiny imagenet visual recognition challenge. In *CS 231N*, volume 7, page 3, 2015.
- C. Li, C. Chen, D. Carlson, and L. Carin. Preconditioned stochastic gradient langevin dynamics for deep neural networks. In *Proceedings of the AAAI conference on artificial intelligence*, volume 30, 2016a.
- C. Li, A. Stevens, C. Chen, Y. Pu, Z. Gan, and L. Carin. Learning weight uncertainty with stochastic gradient mcmc for shape classification. In *Proceedings of the IEEE Conference on Computer Vision and Pattern Recognition*, pages 5666–5675, 2016b.
- Y. Ma, T. Chen, and E. B. Fox. A complete recipe for stochastic gradient MCMC. In *Advances in Neural Information Processing Systems*, volume 28, pages 2917–2925, 2015.
- W. J. Maddox, P. Izmailov, T. Garipov, D. P. Vetrov, and A. G. Wilson. A simple baseline for bayesian uncertainty in deep learning. In *Advances in neural information processing systems*, volume 32, 2019.
- R. M. Neal. *Bayesian Learning for Neural Networks*. Lecture Notes in Statistics. Springer, New York, NY, 1996. ISBN 9780387947242.
- Y. Netzer, T. Wang, A. Coates, A. Bissacco, B. Wu, and A. Ng. Reading digits in natural images with unsupervised feature learning. In *NIPS Workshop on Deep Learning and Unsupervised Feature Learning*, 2011.
- A. Paszke, S. Gross, S. Chintala, G. Chanan, E. Yang, Z. DeVito, Z. Lin, A. Desmaison, L. Antiga, and A. Lerer. Automatic differentiation in pytorch. In *NIPS 2017 Workshop on Autodiff*, 2017.
- R. Shwartz-Ziv, M. Goldblum, H. Souri, S. Kapoor, C. Zhu, Y. LeCun, and A. G. Wilson. Pre-train your loss: Easy bayesian transfer learning with informative priors. In *Advances in Neural Information Processing Systems*, volume 35, pages 27706–27715, 2022.
- J. Von Kügelgen, Y. Sharma, L. Gresele, W. Brendel, B. Schölkopf, M. Besserve, and F. Locatello. Self-supervised learning with data augmentations provably isolates content from style. In *Advances in neural information processing systems*, volume 34, pages 16451–16467, 2021.
- M. Welling and Y. W. Teh. Bayesian learning via stochastic gradient langevin dynamics. In *Proceedings of the 28th International Conference on International Conference on Machine Learning*, ICML, page 681–688, 2011.
- F. Wenzel, K. Roth, B. S. Veeling, J. undefinedwiątkowski, L. Tran, S. Mandt, J. Snoek, T. Salimans, R. Jenatton, and S. Nowozin. How good is the bayes posterior in deep neural networks really? In *Proceedings of the 37th International Conference on Machine Learning*, ICML, 2020.
- A. G. Wilson and P. Izmailov. Bayesian deep learning and a probabilistic perspective of generalization. In *Proceedings of the 34th International Conference on Neural Information Processing Systems*, NIPS, 2020.
- J. Zbontar, L. Jing, I. Misra, Y. LeCun, and S. Deny. Barlow twins: Self-supervised learning via redundancy reduction. In *International Conference on Machine Learning*, pages 12310–12320. PMLR, 2021.
- R. Zhang, C. Li, J. Zhang, C. Chen, and A. G. Wilson. Cyclical stochastic gradient mcmc for bayesian deep learning. In *International Conference on Learning Representations*, 2020.
- R. S. Zimmermann, Y. Sharma, S. Schneider, M. Bethge, and W. Brendel. Contrastive learning inverts the data generating process. In *International Conference on Machine Learning*, 2021.